Supplementary Figure 1

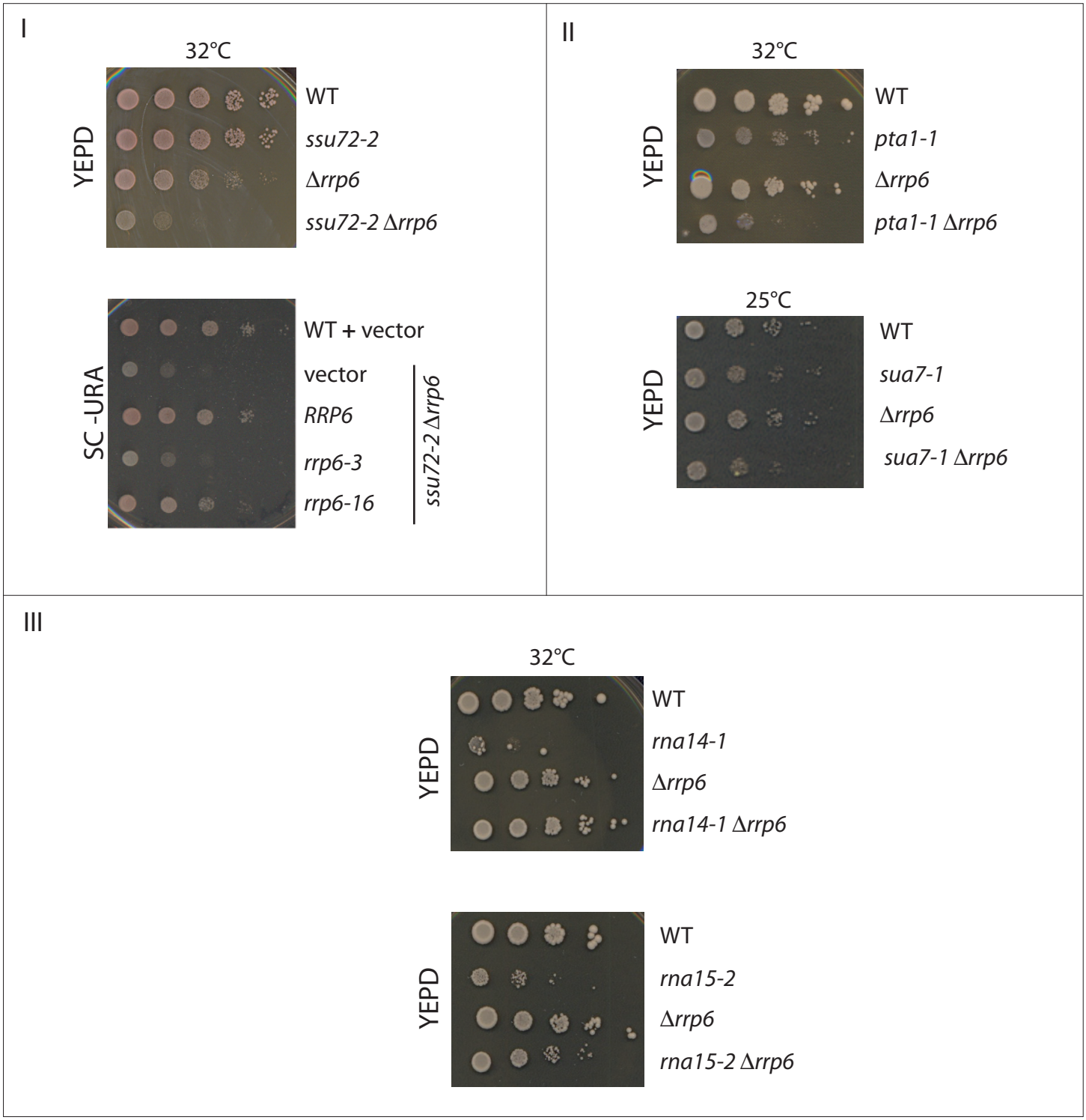

Genetic interaction of *SSU72, PTA1, SUA7, RNA14 and RNA15 with RRP6*. I. WT, *ssu72-2, Δrrp6*, *ssu72-2Δrrp6* strains grown at 25°C (permissive temperature) in liquid YEPD medium (top), or transformed with (*URA3-CEN*) plasmids expressing *RRP6* WT or mutant alleles and grown at 25°C in liquid SC-URA synthetic medium (bottom). 10 fold serial dilutions were spotted on plates with the same media at 32°C (semi -permissive temperature) for 3 days. These results demonstrate *SSU72* genetically interact (synthetic lethality) with *RRP6*. Importantly for *ssu72-2Δrrp6*, cell viability is restored by transformation of *RRP6* or *rrp6-16* expressing plasmids but not *rrp6-3* which is a catalytic mutant in the exonuclease domain. **II.** *PTA1* genetically interacts (synthetic lethality) with *RRP6* (top) as for *SSU72*. *SUA7* (TFIIB) weakly genetically interacts with *RRP6* at 25°C (bottom). S*ua7-1* is a cold sensitive mutant *(31)*. III. *Rna14-1* and *rna15-2* growth defects are both rescued by combined *Δrrp6* mutation. This indicates that loss of Rna15 or Rna14 is compensated by loss of Rrp6 as previously described *(32)*.

Supplementary Figure 2

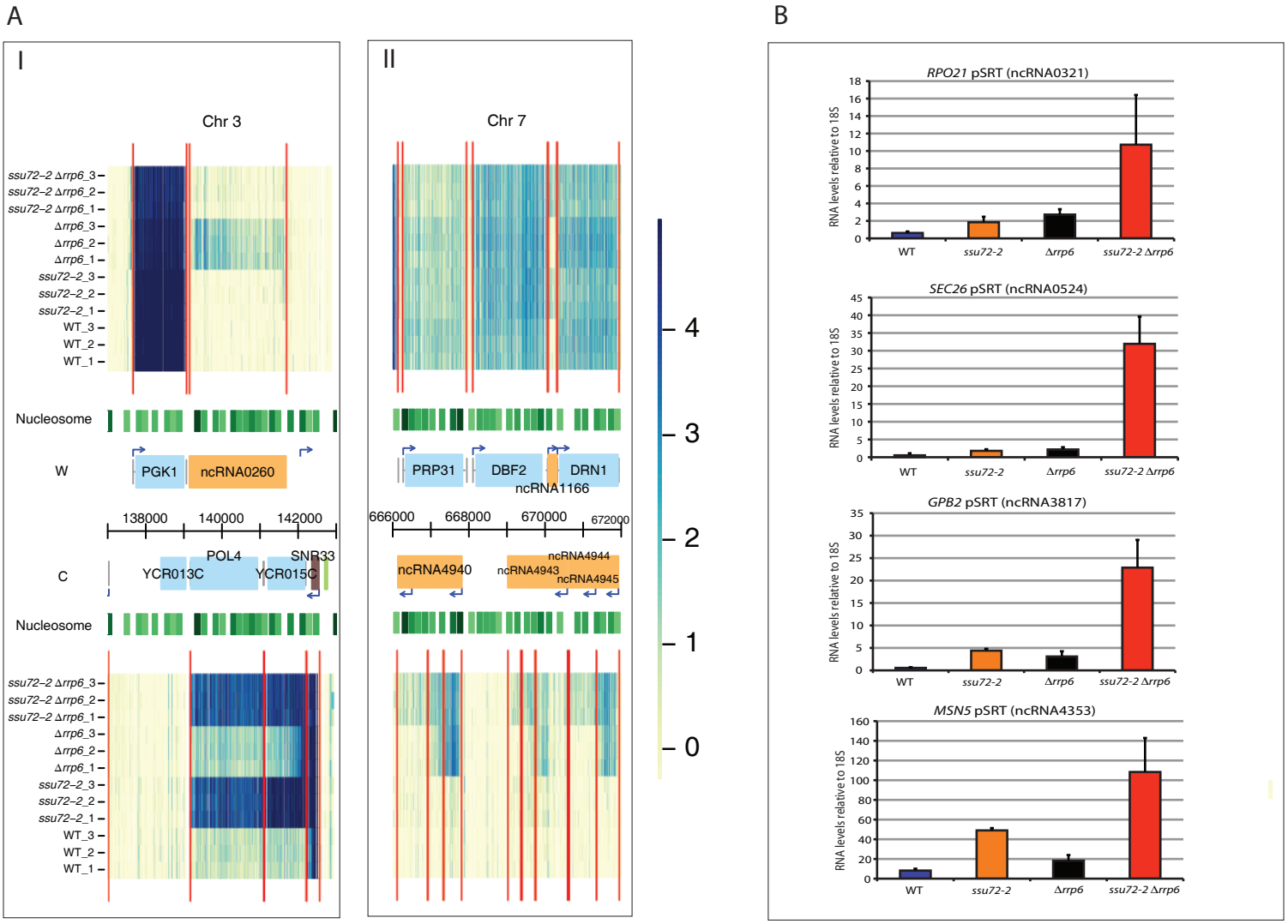

Genomic transcription and validation of by RT-qPCR. Transcription data along 29 kb of chromosomes 3 and 7 (x axis) for the Watson (W, top) and the Crick (C, bottom) strands (Larger views are available for the whole genome in our searchable web database). Three replicates each for the WT (1–3), *ssu72-2* (1–3), *Δrrp6* (1–3) and *ssu72-2 Δrrp6* (1–3) strains were grown in YEPD media at 32°C. Normalized signal intensities are shown for the profiled samples (y axis). Red vertical lines represent inferred transcript boundaries. Nucleosome positions (green tracks, darker for more significant scores) and genome annotations are shown in the centre: annotated ORFs (light blue boxes) ncRNAs (orange boxes), and transcript start sites (arrows). **A I**. Ssu72 inactivation leads to majority of extended snoRNA transcripts presumably resulting from read-through of normal transcription termination. snR33 is shown as one example. **A II** Ssu72 inactivation leads to extension of most CUTs presumably resulting from a read-through of normal transcription termination. ncRNA4940 to ncRNA4945, crick strand are extended in the double mutant *ssu72-2 Δrrp6* as compared to *Δrrp6* alone. These transcripts are the extended versions of the previously characterized CUT611, CUT613 and CUT614 cryptic unstable transcripts (http://steinmetzlab.embl.de/NFRsharing/). **B**. RT-qPCR results validating the expression of 4 pSRTs that were identified using tiling arrays. RNA extracts from WT, *ssu72-2, Δrrp6* and *ssu72-2Δrrp6* strains were analysed in triplicate using gene specific primers for the RT (Table S1). The relative expression values were normalized to 18S rRNA. Error bars represent SEM.

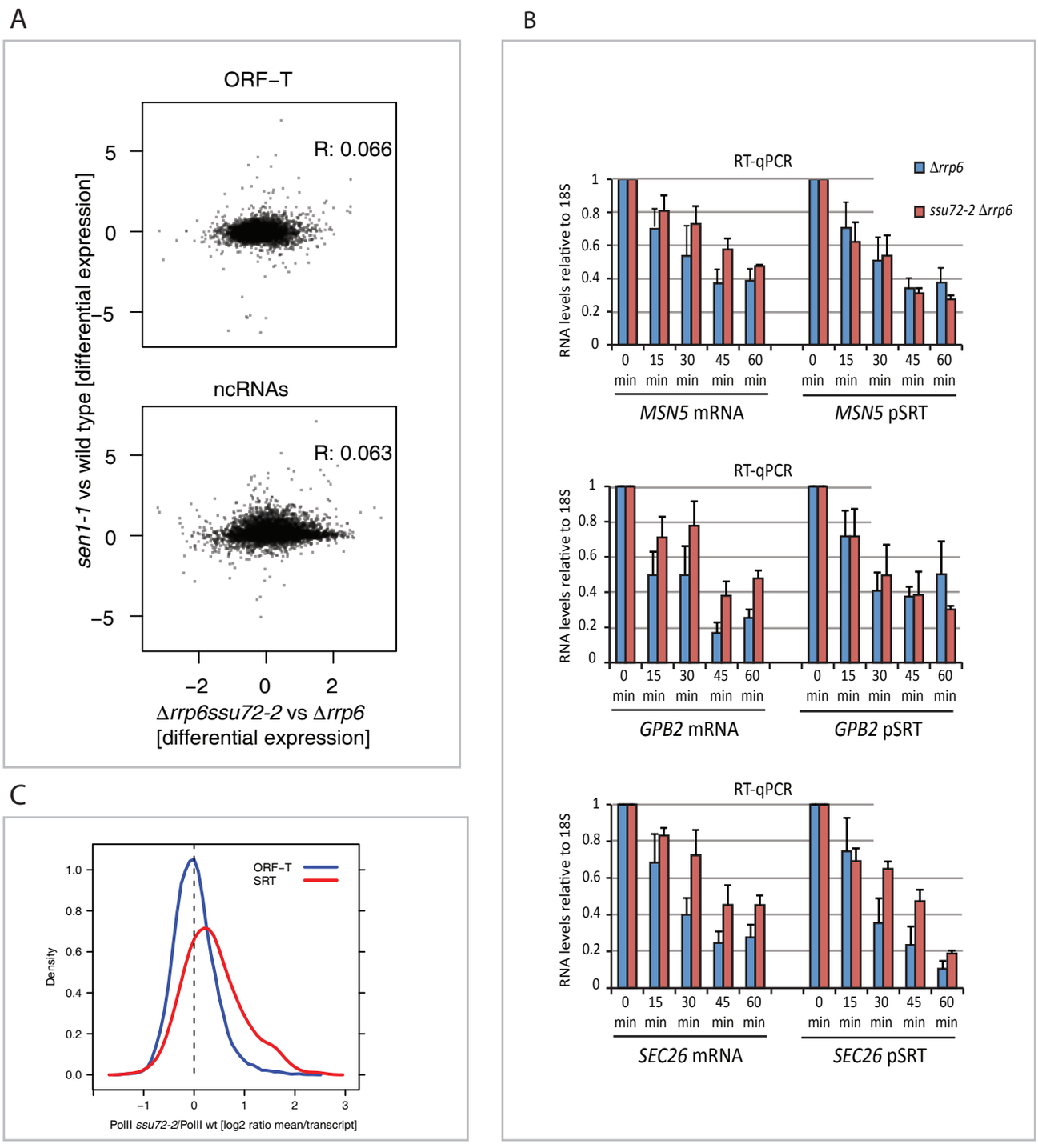

SRTs are promoter associated transcripts and do not derive from RNA stability or increased transcriptional read through.

A. Sen1 inactivation does not enhance SRT expression. Differential expression *ssu72-2Δrrp6* vs *Δrrp6* is plotted against *sen1-1* vs wild type for both ORFs (top) and ncRNAs (bottom). The pearson correlation coefficient (R) is <0.1 in both cases, signifying that our SRTs (expression in *ssu72-2Δrrp6*) are independent of *sen1-1* vs wild type expression. This indicates that SRT increased expression resulting from Ssu72 inactivation is not in general due to inefficient NRD dependent transcription termination.

B. Increased pSRT levels do not result from increased RNA half-life. Measurement of RNA decay in *Δrrp6* and *ssu72-2Δrrp6* strains for *MSN5, GPB2* and *SEC26*. In detail *MSN5* and *GBP2* showed a similar drop in RNA levels for their mRNA and pSRTs over a 60 min time course of thiolutin inhibition. For *SEC26*, both mRNA and pSRT showed equivalent increased instability for the *ssu72-2Δrrp6* versus *Δrrp6* alone. However there was no differential change in pSRT stability versus mRNA. Cells were grown at 32 °C in YEPD and transcription was blocked by addition of thiolutin (25mg/mL). Samples were then taken every 15 min, RNA extracted and then mRNA or pSRT expression was measured by RT-qPCR using gene specific primers for RT (Table S1). Error bars represent SEM.

C. SRTs show increased Pol II binding in ssu72-2 mutant vs wild type than ORFs. Differential Pol II binding between *ssu72-2* and WT is calculated as the difference in mean occupancy across the entire transcripts as annotated in this study.

A

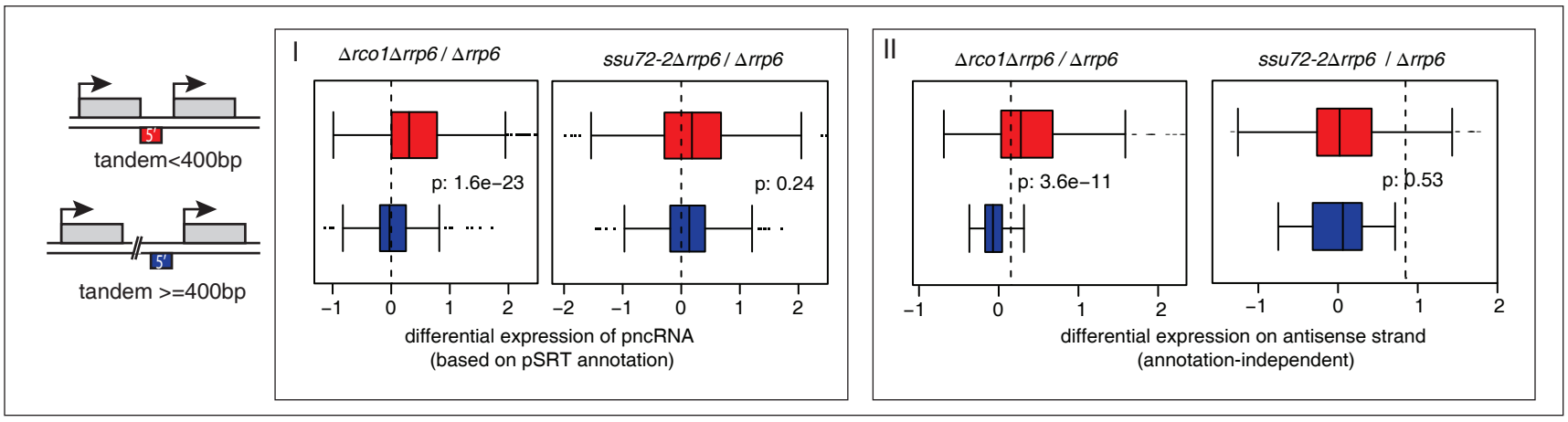

Δ*rco1* increases antisense transcripts emerging from the 3' end of a gene whereas *ssu72-2* increases promoter associated transcripts, (I) annotation-based and (II) annotation-independent analysis. To determine whether *ssu72-2* and Δ*rco1* result mainly in 3' or 5' transcription, we compared the differential expression of **(I)** pSRT regions and **(II)** independent of any annotation, regions between tandem genes 200-400bp of the downstream gene's TSS for different gene configurations: close tandem genes (red) and far apart tandem genes (blue). For the annotation-independent analysis we selected all tandem gene pairs and calculated the mean differential expression level on the antisense strand 200-400bp upstream of the TSS of the downstream gene. P-values are reported for each pair of configurations (Wilcoxon rank sum test). When comparing *ssu72-2*Δ*rrp6* and Δ*rrp6*, we find no difference in ncRNA expression in pSRT regions between tandem ORFs that are close or far apart, indicating that the transcripts emerge from the promoter regions. For Δ*rco1*Δ*rrp6 vs* Δ*rrp6* expression however, the ncRNAs show increased expression in the Δ*rco1*Δ*rrp6* vs Δ*rrp6* only for the close tandem genes, indicating that RRTs arise from the upstream 3' region of the tandem genes. This is true for both, the pSRT-annotation based (I) and the annotation-independent analysis (II).

B

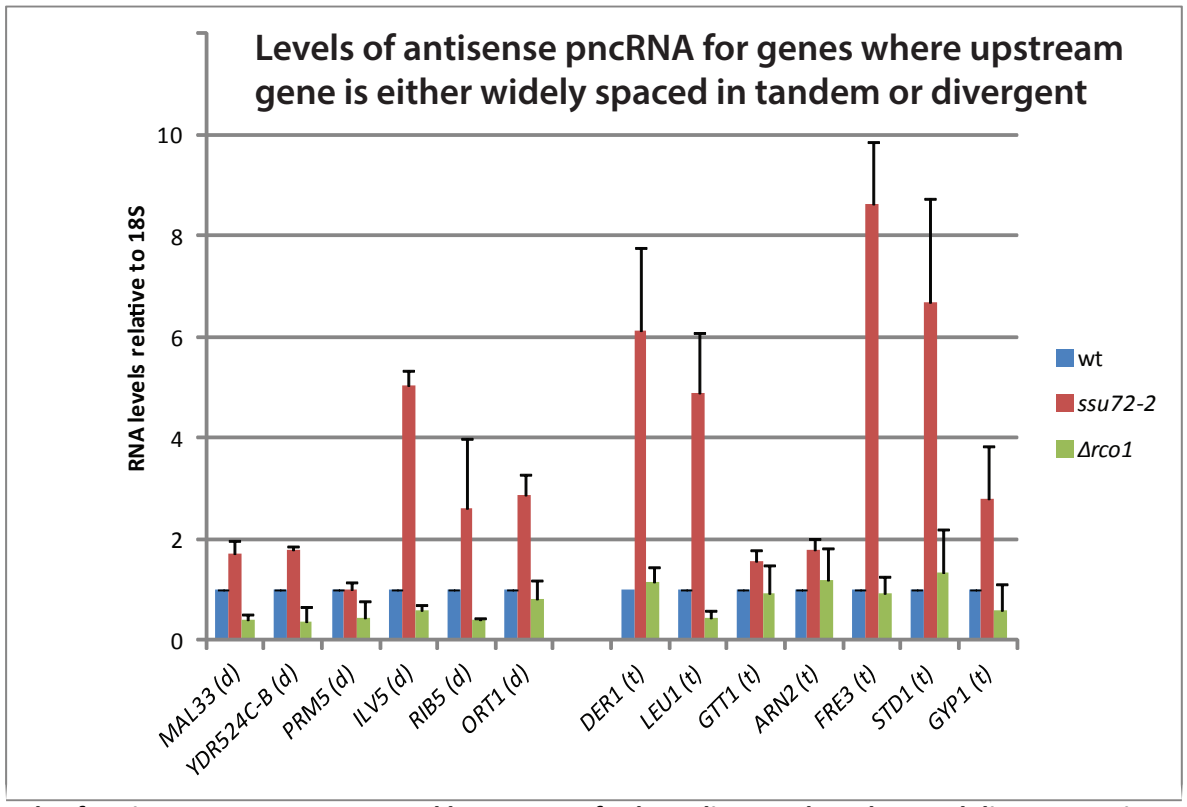

Levels of antisense pncRNA measured by RT-qPCR for long distanced tandem and divergent orientated gene pairs. RT-qPCR results validate the expression of pSRTs shown on tiling arrays for long distanced tandem (t) (more than 400bp of intergenic regions) and divergent (d) orientated gene pairs. RNA preparations from WT, *ssu72-2, Δrco1* strains were analysed in triplicate using gene specific primers for the RT (Table S1). Relative expression values were normalized to 18S rRNA. Most selected pncRNA displayed elevated transcript levels in *ssu72-2* but not in *Δrco1* when compared to WT. Error bars represent SEM.

C

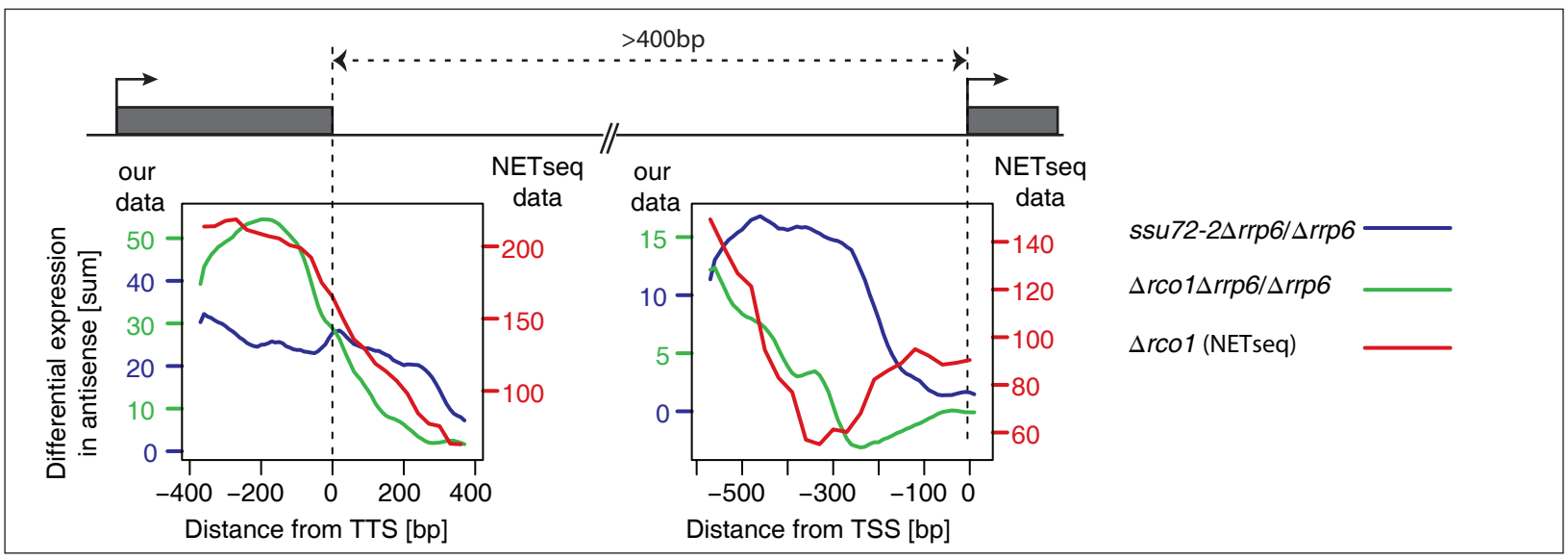

Comparison with published *Δrco1* mutant data from a NETseq study: RRTs accumulate at gene 3' ends while SRTs accumulate at 5' ends. SRT (blue) and RRT (green) levels were calculated as described in Figure 2c. NETseq data for the *rco1* mutant was taken from *(7)*. For calculating the differential expression of the NETseq data we summed the reads in 30bp bins and calculated the log ratio of reads in Δ*rco1* and WT. These values were then plotted relative to the genes TSS or TTS and smoothed using a moving average (window size = 150). Different scales were used for our data (blue/green scale on the left) and the NET seq data (red scale on the right). There is a very strong correspondence between our Δ*rco1*Δ*rrp6*/Δ*rrp6* and the NETseq Δ*rco1* data, indicating that the conclusions drawn from our study also apply to the data from *(7)*.

Supplementary Figure 5

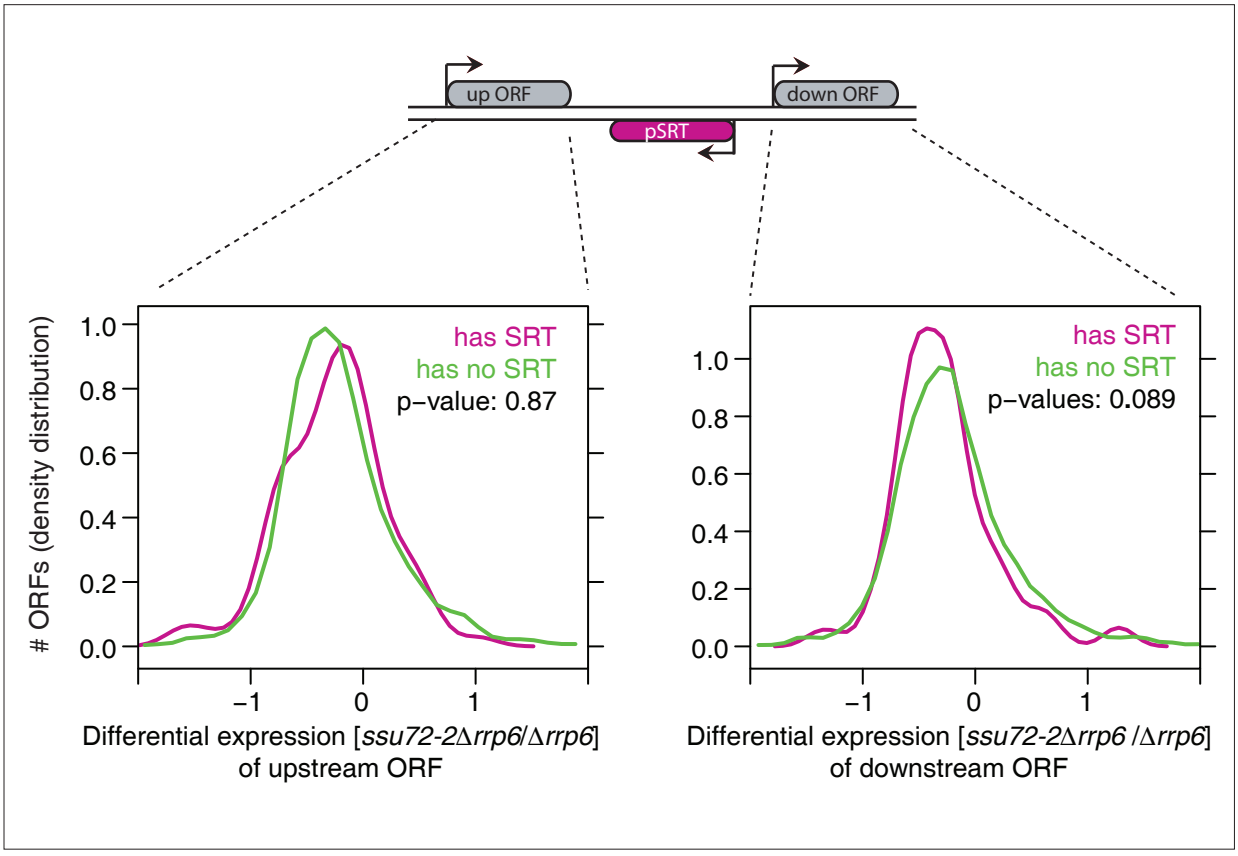

ORFs that generate divergent SRT are down regulated. Differential expression in *ssu72-2Δrrp6* over *Δrrp6* is shown for the upstream (left) and downstream (right) gene of tandem gene pairs that are separated into whether they have a SRT (red) or no ncRNA transcript (green) emerging between them (see schematic). We observe no expression level difference for the upstream ORF, indicating that pncRNA do not affect the ORF by antisense inhibition mechanism. However, for the downstream ORF, we find a small but significant reduction in the expression for ORF that have associated SRT. This indicates that loss of transcriptional directionality might impact on the ORF by lowering its expression level. P-values are given for the pairwise wilcoxon rank sum test.

Supplementary Figure 6

A

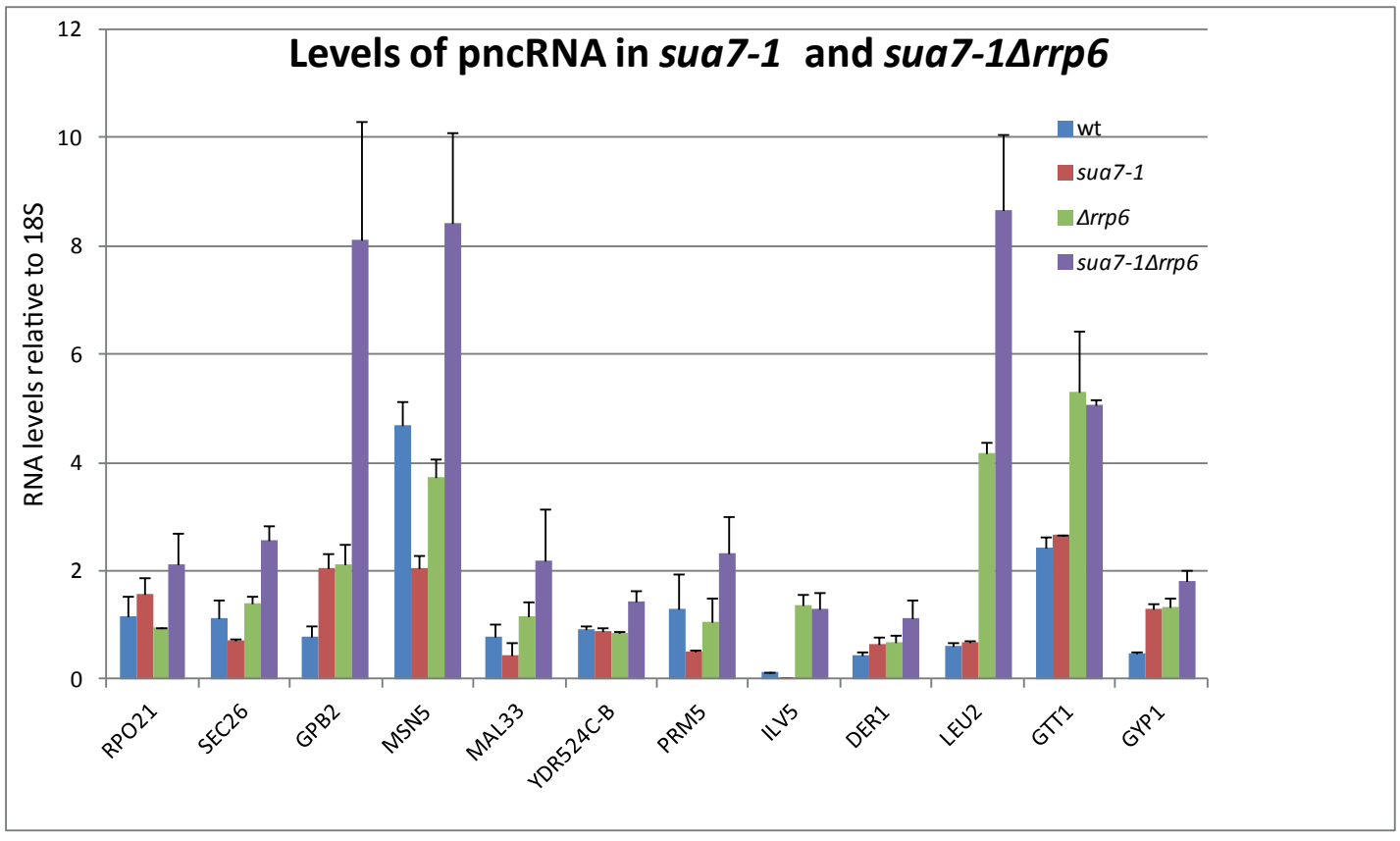

B

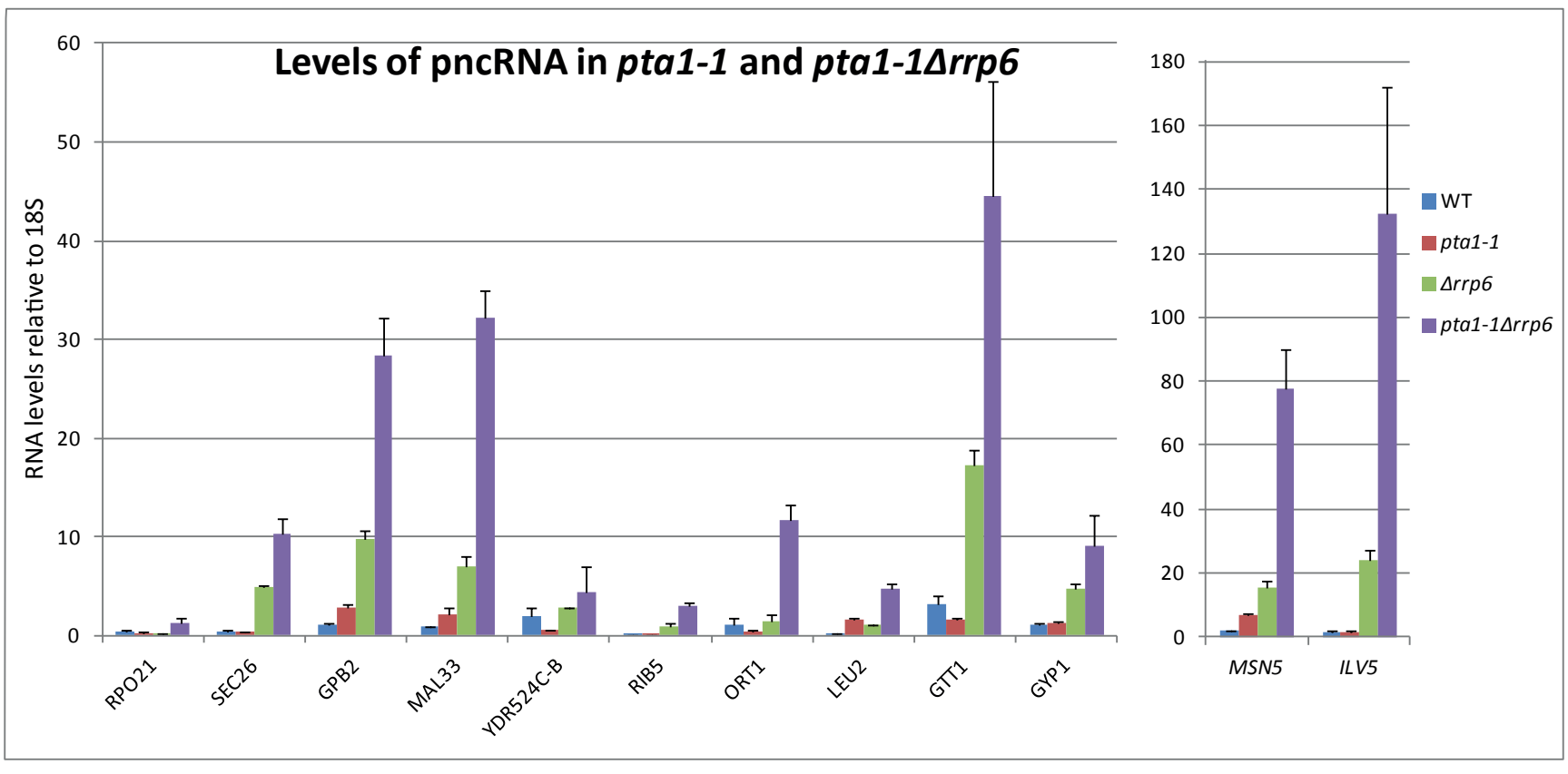

Supplementary Figure 6

C

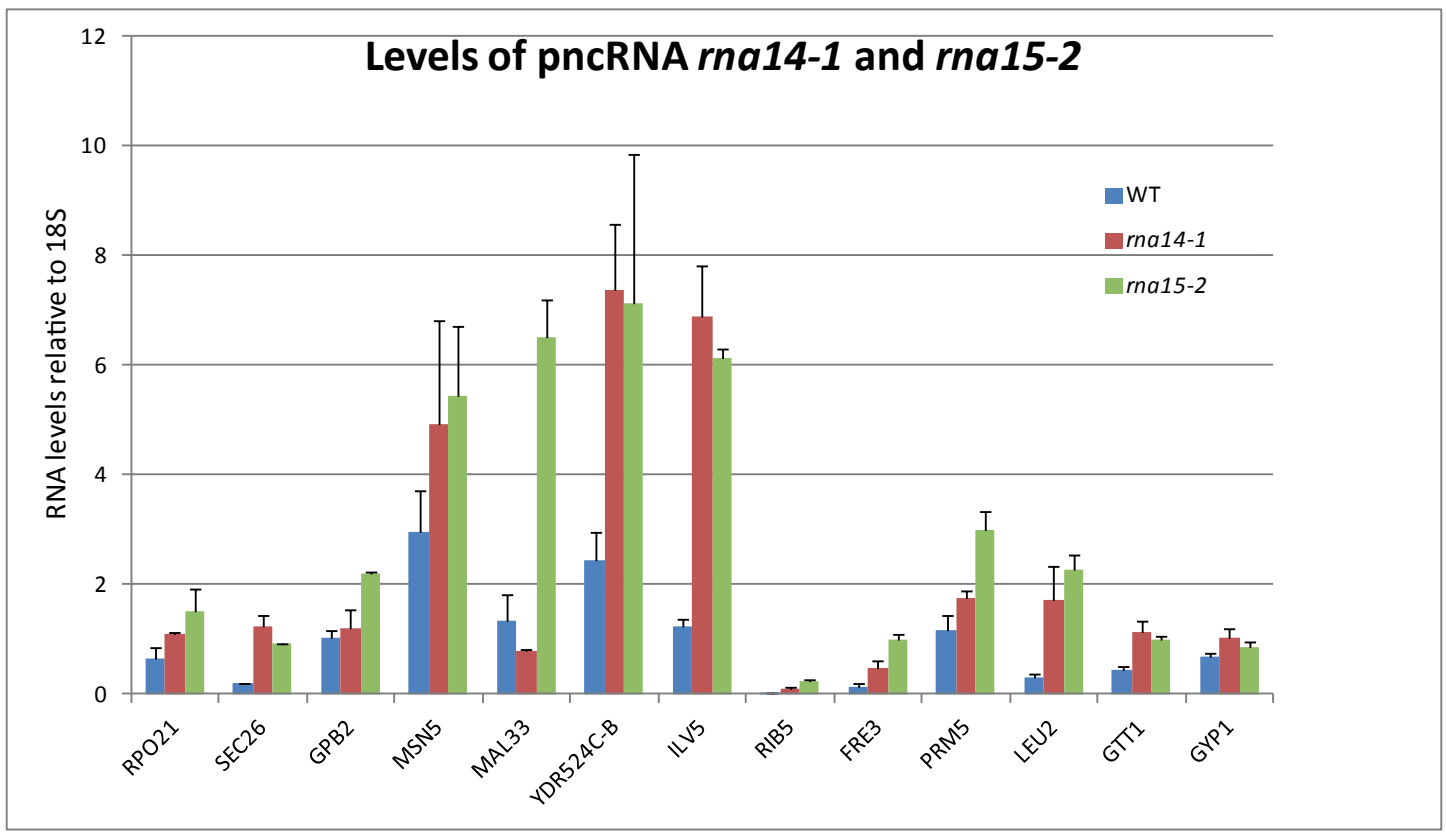

D

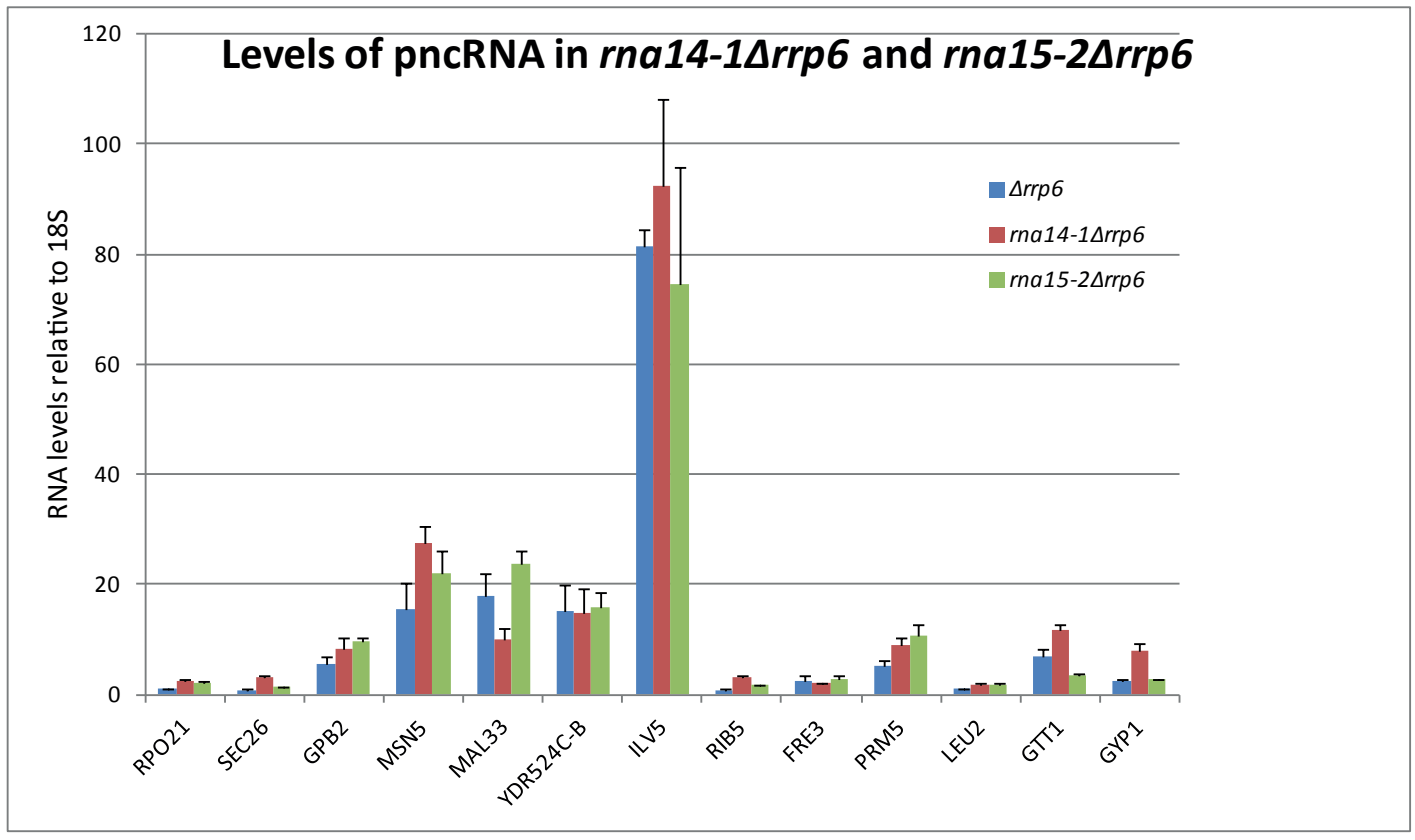

Levels of antisense pncRNA measured by RT-qPCR in *sua7-1, pta1-1, rna14-1, rna15-2* and their respective *Δrrp6* double mutants. RT-qPCR used to measure expression of pSRTs. RNA preparations from strains listed above and their isogenic WT were analysed in triplicate using gene specific primers for the RT (Table S1). Relative expression values were normalized to 18S rRNA. Most selected pncRNA displayed elevated transcript levels in *sua7-1Δrrp6, pta1-1Δrrp6 t*o WT or *Δrrp6* whilst *rna14-1* and *rna15-2* single mutants displayed elevated transcripts. These results are consistent with the genetic interaction data (Fig. S1). Thus *ssu72-2* and *pta1-1* were synthetic lethal with *Δrrp6*, pncRNA activation was therefore highest with double mutants. For *sua7-1* weak genetic interaction was observed with *Δrrp6*. Similarly *sua7-1Δrrp6* generally made more pncRNA that *sua7-1* alone. Finally, *rna14-1* and *rna15-2* showed elevated pncRNA levels as compared to WT but gave similar levels of pncRNA when combined with *Δrrp6* to *Δrrp6* alone. Overall these results show that with *SSU72, PTA1, SUA7, RNA14* and *RNA15* display different genetic interaction behavior with *RRP6*. However, it is clear that all of these genes when mutated generate higher levels of pncRNA. This correlates with the known requirement of all of these encoded factors for gene loop formation *(9-11).* Error bars represent SEM.

Supplementary Materials and Methods

Website:
The website (http://steinmetzlab.embl.de/proudfoot_lab/index.html) provides further information as well as an interface to visualize tiling array expression data.

Plasmids and yeast strains
RRP6::KANMX4 and *RCO1::KANMX4* gene deletion was transferred from BY4147 to W303 background by the transformation of PCR fragments generated with primers listed in Table S5. *RRP6* and *GAL-CYC1* plasmids were previously described (*21, 26*). *MSN5* PAS site replacement with RCS was created using a so called "pop-in pop-out" technique with a long flanking homology double PCR procedure (*27*). In brief, in each step, two main PCR reactions were performed. First, Short Flanking Homology (SFH) PCR was performed on *MSN5* with primers designed to delete 20 bp of pA site and also contain an immediate ~20 bp overhang of *URA3* homology from either the 5' or 3' end. Secondly, the products of these SFH PCR reactions (at about ~500 bp each) were then used as primers for the second step Long Flanking Homology (LFH) on a *URA3* template. This produced the *URA3* module flanked by about 500 bp *MSN5* homology sequence without the *MSN5* 20 bp PAS. This *MSN5URA3* LFH PCR product was transformed into *Δrrp6* (W303) strain and selected on SC-URA plates to produce a popped-in *URA3* selectable marker. The whole LFH process was repeated but with primers designed with overhanging RCS sequence. The resulting *MSN5RCS* LFH PCR product was then transformed into the "pop-in" *MSN5URA3* strain and selected on SC-FOA plates. Transformants obtained were screened for the "pop-out" *URA3* marker and the "pop-in" RCS sequence. Primers are listed in Supplementary Table 6.
HEK293 Flp-In T-Rex Expression Cell Line containing integrated pcDNA5/FRT/TO/βwt and pcDNA5/FRT/TO/βpAmut were very kind gifts from Torben Jensen (Aarhus University, Denmark). β-globin gene expression was induced by treating the cells with 250 ng/ml Tetracycline overnight (16 hrs) after EXOSC3 knockdown as described previously (*4*).

RNA analysis by RT-qPCR
Total RNA was extracted with hot phenol procedure and analysed using gene specific primers by RT-qPCR (*26*). Primers used for RT-qPCR are presented in Table S1.

RNA analysis by Northern blot
Total RNA was extracted using the hot phenol procedure and analysed by Northern-blot using riboprobes. Samples were run in a 2% agarose gel and transferred into a positively charged Hybond-N^+ membrane (Amersham). Riboprobes were prepared with an *in vitro* transcription kit (Ambion). Primers used to produce the T7 PCR product are described in Table S4.

Chromatin immunoprecipitation analysis (ChIP)
ChIP experiments were performed using standard procedures (*28*). Primers used for real-time PCR are described in Table S2.

Chromosome Conformation Capture analysis (3C)

3C experiments were performed following standard procedures (*28*). Briefly, 1X 10^7 cells were cross-linked with 1% formaldehyde. DNA was subsequently digested with 800 U restriction enzyme (*Sty*1 for *FMP27*, *Nla* III for *CYC1* and *Hae*III for *MSN5* and β-globin) and ligated at 2.0-2.5 ng/µl. Chromatin was reverse cross-linked with proteinase K (30µg) at 65^{o}C and DNA purified (Qiagen PCR purification column). For *CYC1* and *MSN5*, 3C interactions were fractionated on agarose gels and were quantified with Gene Tools Syngene (Gene Genius Bioimaging System) and standardized to relative primer efficiency and loading values. In mammalian β-globin and yeast *FMP27* experiments, 3C Taqman qPCRs were performed using SensiMix DNA Kit (Quantace) with cycle conditions as follows; 95^{o}C 10 min; 45x (95^{o}C 15 sec, 60^{o}C 60 sec). Taqman reactions were performed with a 5'FAM and 3'BHQ-1 dual-labled probe and primers designed by the Primer Express software (Applied Biosystems). The dual-labelled probe was used at 333 nM, and primers at 167 nM final concentrations. Primers are described in Table S3.

Tilling array using total RNA samples

All strains were grown in 200 ml of YEPD media at 32°C (OD_{600} ~ 1.0). Total RNA was isolated by the standard acidic hot phenol method. For each sample 20 µg total RNA was annealed with 1.72 µg random hexamer and 0.034 µg oligodT copied by Superscript II reverse transcriptase and then treated with RNase-free DNase I using Turbo DNA-free kit (Ambion). For first-strand cDNA synthesis, 9 µg of polyA+ RNA was mixed with 4.5 µg of random hexamers, 0.09 µg of oligodT and incubated at 70°C for 10 min, then transferred to ice. The synthesis included 2,000 U SuperScript II, 50 mM Tris-HCl, 75 mM KCl, 3 mM MgCl2, 0.01 M DTT, 0.25 mM dNTPs mix (Invitrogen), 6.25 µg/mL actinomycin D in a total volume of 200 µL at 42°C for 1 hr. Samples were then subjected to RNase treatment of 20 min at 37°C (30 units RNase H, Epicentre, 60 U RNase Cocktail, Ambion). First-strand cDNA was purified by standard phenol extraction using Phase Lock Gels (PLG) (1.5 mL light, Eppendorf), ethanol precipitated and washed twice with 80% ethanol. The sample was dissolved in DEPC water and 4.5 µg were digested by using 0.1 U DNase I (Invitrogen) in 1xOne-Phor-All buffer (Amersham Pharmacia) and 1.5 mM $CoCl_2$ (Roche) solution at 37°C, to yield fragments of 50-100 bp in size. Each sample was 3' end-labeled with 0.07 mM Biotin-N6-ddATP (Enzo Life Sciences) using 400 U of Terminal Transferase (Roche) for 2 hr at 37°C.

Hybridization to arrays

The labelled cDNA samples were denatured in a solution containing 100 mM Mes, 1 M [Na+], 20 mM EDTA, 0.01% Tween-20, 50 pM control oligonucleotide B2 (Affymetrix), 0.1 mg/ml herring sperm DNA, and 0.5 mg/ml BSA in a total volume of 300 µl, from which 220 µl were hybridized per array. Hybridizations were carried out at 45°C for 16 hr with 60 rpm rotation.

Manual curation of transcripts and transcript boundaries

Manual curation of the automated segmentation results was necessary because the automated segmentation algorithm used to detect transcript boundaries often over-segmented contiguous transcripts. In particular, although random priming during reverse transcription provides cleaner hybridization signals than oligodT priming, it also systematically yielded reduced hybridization signals at transcripts 3' ends, which leads to a violation of a modelling assumption underlying the algorithm, the assumption of piecewise constant signal along the genome. Consequently the automated segmentation results were insufficient to accurately detect 3' transcript boundaries. Moreover, condition-specific 5' and 3' ends violate the assumption of constant signal across

conditions and are easily misidentified by the automatic segmentation. A webserver was created for interactive manual curation. Data were stored in a MySQL database and a web interface based on the Scalable Vector Graphics (SVG) technology allowed the display and edition of the segment boundaries by the curators.

Definition of SRTs

We considered a minimum of 2-fold expression increase in *ssu72-2Δrrp6* expression over *Δrrp6* alone, as indicative of an SRT. Transcripts with increased expression in *ssu72-2* mutant vs. WT but not the double mutant vs. *Δrrp6* were classified according to their expression in *Δrrp6* vs. WT (CUT ncRNA 0150; Fig. 2AI). We evaluated this cut-off placement by analyzing the significance of expression changes using three biological replicates. By performing a moderate t-test we found that a 2-fold difference is a stringent cut-off in terms of significance

Definition of tandem ORFs and pncRNAs

Tandem ORFs were defined as two consecutive ORFs that lie on the same strand. Upstream and downstream are defined relative to the ORFs so that on the + strand the upstream ORF would be the one on the left and the downstream ORF on the right. Promoter associated (p)ncRNAs were defined as ncRNAs that emerge between two tandem ORFs with opposite polarity. They are called pncRNA because they are always divergent to an ORF.

Additional genomic data

H4 Acetylation data were obtained from (*15*). We calculated the average H4 acetylation as reported in regions between the TSS of the ORF and the corresponding cryptic transcript (CUT or SRT). Difference in H4 acetylation in CUTs and SRTs was then tested with the wilcoxon rank sum test. We also tested maximum levels instead of the average and find they are significantly different as well (p=4.9e-12). Additional genomic data was processed in the same way.

Comparison of Δ*rco1* and *ssu72-2* (Fig. S4A)

The analysis is based on the pncRNAs (as defined above) that have been manually annotated in *wild type, Δrrp6, ssu72-2 and ssu72-2Δrrp6* in this study. The probe levels were averaged across each transcript and compared between tandem genes that are close or far apart from each other (Fig. S4AI). To ensure that these values were not biased due to the fact that we did not use *Δrco1Δrrp6 vs Δrrp6* for annotating the transcripts we also performed an annotation-independent analysis were we compared the average differential expression 200-400 bp upstream of the TSS of the downstream ORF (Fig. S4AII). We found that the difference for the *Δrco1Δrrp6 vs Δrrp6* in close vs distant tandem genes was the same in the annotation-based (Fig. S4AI) and the annotation-independent (Fig. S4AII) case and therefore concluded that there is no annotation-dependent bias.

Metagene analysis (Fig. 3B)

The metagene analysis in Fig. 3B is based on pncRNAs (as defined above) that arise between two tandem genes that are at least 400 bp apart from each other. The annotation of the transcripts was taken from this study based on the wild type, *Δrrp6 ssu72-2Δrrp6* mutants. The probe levels were averaged across each transcript and aligned to either the TTS of the upstream ORF or the TSS of the downstream ORF. We then summed the differential expression for the different mutants at each position from the TTS or TSS respectively and plotted this value in Fig. 3B.

Comparison with NETseq data
NETseq data were obtained from (*16*) For the comparison in Fig. S4C we calculated the log-ratio of the sum of reads falling in pncRNAs based on the annotation in this study for *Δrco1* and WT.

Determination of Sen1 role in SRTs expression (Fig. S3A)
Since with *ssu72-2*, many ncRNA transcripts display read-through profiles, especially for CUTs, we also considered the possibility that pSRTs derive from read-through transcription due to defective CUT termination. We tested whether mutation of Sen1 a component of the NRD complex which is required for CUT termination (*29*) displays a similar profile of new ncRNAs as seen with *ssu72-2*. Transcription analysis of WT versus *sen1-1* (Fig. S3A) (*30*) indicated that pSRTs reflect *de novo* bidirectional promoter activity rather than defective NRD mediated termination.

Supplementary Tables

Table 1: Primers for RT-qPCR

FMP27 F (amplicon B)	AGATGGTACCGTCAGGCTAA
FMP27 R (amplicon B)	CCATTGAGCCAGTATTGTGA
FMP27 ncRNA F (amplicon A)	GCTCTTTTTTCCTCCTCCTCT
FMP27 ncRNA R (amplicon A)	CGCAATGTTTTCTTCATTGA
RPO21 SRT F	CGTTAGCCCAAAGAGTATATTCATC
RPO21 SRT R	AATATACGGCATTTTAGCACCT
SEC26 SRT F	TCTCCAACGCCAGTAATTTCT
SEC26 SRT R	TTTACAAGCGCCTCCTAACTT
SEC26 ORF F	GGTGAAGATGCTCGTTATGTTA
SEC26 ORF R	CCATATTAGTTCCCTTGACCA
GPB2 SRT F	GTGGCTCAAAATTGACCTTT
GPB2 SRT R	GCCATCAATAAGGTTGACAA
GPB2 ORF F	GATGATATGTGGTTGATGGACTT

GPB2 ORF R	CGAGTAAAATTGGTCAACATCCT
MSN5 SRT F (and amplicon A)	CATGGCTAAGTTTGCAGCTT
MSN5 SRT R (and amplicon A)	GAAAATGCTTCAGGTGGAG
MSN5 ORF F (and amplicon B)	TGTGCTGTGTAATAGTGCGTTTA
MSN5 ORF R (and amplicon B)	GTTTTGTATTCGTCCACGCT
CYC1 F (amplicon C)	TGGCAGACACTCTGGTCAAG
CYC1 R (amplicon C)	AAGGGGCCTGTTTACTCACA
pRS424 F_2 (amplicon B)	GAATTGCTTGTGATATTGACGA
pRS424 R_2 (amplicon B)	GCCAATGAAAGATGTATGTAGATG
pRS424 F_1 (amplicon A)	ATTATTGAAGCATTTATCAGGGTT
pRS424 R _1(amplicon A)	GGTTAATGTCATGATAATAATGGTTTCT
β-globin ex3 F (amplicon B)	CAAAGAATTCACCCCACCAG
β-globin ex3 R (amplicon B)	AGACCCAGTTTGGTAGTTGG
β-globin ncRNA F (amplicon A)	AATACATTCAAATATGTATCCGC
β-globin ncRNA R (amplicon A)	ACCGCGCCACATAGCAGAAC
18S F	GATGCCCTTAGACGTTCTGG
18S R	GGCCTCACTAAGCCATTCAA
MAL33 SRT F	GTTCCAATCAGTCCCATTC
MAL33 SRT R	TACTGTGAATTCAACAAACCA
YDR524C-B SRT F	TCGCTATTTTGGAAATAAACT
YDR524C-B SRT R	CTGCTTATTTCCCGAGAATAC
PRM2 SRT F	GATCAGATAGCATTAATAGCGTG
PRM2 SRT R	GTCTCAATATAACCGGTCACC

ILV5 SRT F	AGTTCACCACGTAATGCCT
ILV5 SRT R	ATTCTGTATCCCTAAATAACTCC
RIB5 SRT F	GATGGATCTGGAATATGACTAA
RIB5 SRT R	TGTTCAAGCTCGCTGTAA
ORT1 SRT R	CATTGTATCCATTAATATGGTCC
ORT1 SRT R	TCAAAGACAGTATTATCCACACTT
DER1 SRT F	CAGCGCCACAATGAAATCTA
DER1 SRT R	AGCCAAATATTTCCACTCAAT
LEU1 SRT F	CTGGAAACTTGTAGAATGGC
LEU1 SRT R	TGGAAGTCTCGCTTACGTTTA
GTT1 SRT F	CCCAAGGGAGCTTACAC
GTT1 SRT R	AATGCAGTTCATGGGCAC
ARN2 SRT F	AAGCTCATCTCAAACAAACAG
ARN2 SRT R	GGTACTTCCATAACTACATAATCAT
FRE3 SRT F	TGAGCAACTGGATTCGATCA
FRE3 SRT R	AACCCTCGATCACCCAAAAT
STD1 SRT F	GTAGTGCCGTATTCGAAACTT
STD1 SRT R	TGCTGAAGCATGAATATATGA
GYP1 SRT F	TTATCGCCATGAGCCTTAG
GYP1 SRT R	GGTGATCACTTAGGTAACAATC

Table 2: Primers for ChIP analysis

SEC26 F	AGCTCGACAAGTGAAATTTGA
SEC26 R	CGGTACTCGAGTAAGTCTCCATACT
GPB2 F	TCGCATTACTAAATCATAGGCAT
GPB2 R	AAAGGTTCAAAGCAATGATCA
RPO21 F	CTGATCGACTCTCTTTGTTAGTTTT
RPO21 R	ATCAGGGAATTCGCTAGGAA
MSN5 F	CGCGATCAAGGTTGGTTTTT
MSN5 R	GCTCAACGAATAAAGATAGGCTAAA
TELVI F	TCCGAACTCAGTTACTATTGATGGAA
TELVI R	CGTATGCTAAAGTATATATTACTTCACTCCATT

Table 3: Primers for 3C analysis

Taqman probe *FMP27*	TCAGGTAGTTGCTGGAACATGAAGTCGCT
Anchor *FMP27* F_1	CTAATATGGCTAAATGTTTGAGACAGAAG
FMP27 F_2	AGGGTTTTGGGATAAAACAAGATATC
FMP27 F_3	AACGCCGTTTGATAATCGTGTC
FMP27 F_4	CTCCAGCTCATATGGCCAAGA
FMP27 F_5	TTCAGACCTTTATTGCTGTACTACATTG
FMP27 F_6	AGCAGCAAAATTAAACTATTCGGAC
FMP27 F_7	TGCAAAGTTGGCTCGTTTCC
CYC1 F_2	TTTGGCAGACACTCTGGTC

CYC1 F_3	TTCCTGGTACCAAGATGGC
CYC1 F_4	TGTTTTCCTTAGTAGCGTCTG
CYC1 F_5	CATTCCAGTTTAGTTGTCGACTGATA
CYC1 F_6	TTGACTTCATCGAGACTTTCA
CYC1 F_7	ACCCACCTGCACTCAAAGAA
CYC1 F_8	TCCTCCCTGAAATGTTCAAAC
CYC1 F_9	CTTACAAAAAGAACAGTACCGTCG
Anchor *MSN5* F_1	TCTCAACGGCAAGAAGCTCAG
MSN5 F_2	GATTGTTTGCCCTATTGAAGTT
MSN5 F_3	CCGTCCCTATAGTAATGAAAG
MSN5 F_4	AAGATCTGTGGAGACCTAGGATTGT
MSN5 F_5	CATTGGCAATGGAACAACTGT
MSN5 F_6	GTCGATTGTTGGAAGGAAT
Anchor *β-globin*	TCCTGAGGAGAAGTCTGCCGTTA
β-globin F_2	TGCTCGGTGCCTTTAGTGATG
β-globin F_3	TAAGGCTGGATTATTCTGAGTCCAA
β-globin F_4	CACCCATGTCTGCTGTCTAGAGG
β-globin F_5	GAACTTCAAGCTTGGCACTGG
β-globin F_6	AACCATCCGCTGTGGTACA
β-globin promoter probe	ATCCACGTTCACCTTGCCCCACAG

Table 4: Primers for Northern blot riboprobes

CYC1 T7 R	TAATACGACTCACTATAGGGAGAAAGGGGCCTGTTTACTCACA

CYC1 F	TGGCAGACACTCTGGTCAAG
pRS424 F_2 T7 R	TAATACGACTCACTATAGGGAGAGCCAATGAAAGATGTATGTAGAT
pRS424 F_2 F	ATTATTGAAGCATTTATCAGGGTT

Table 5: *RRP6* and *RCO1* deletion primers

RRP6 -500 R	GCATCATAAGAGCATAAGCGAC
RRP6 +500 R	CTATGCGAAGCCTGATGTGAAG
RRP6 +600 R	GCTGGTTTGTTCACCAGTAACCT
RCO1 -500R	GTTCTCCTTGTAGAACCACAA
RCO1 +500R	ATTCTTCACACGTCACAAACT
KANMX4 3'end F	GCCTCGACATCATCTGCCCA

Table 6: MSN5 RCS replacement primers

5'*MSN5*US	TTGACTCTGTGCAAAGAATATC
5'*MSN5URA3*R	TTCCTTCTGCTCGGAGATTACATGACTATTTGCTTTCTCTA
3'*MSN5URA3*F	GCCAGAACCAAGTAACAGTATAATTATTGTGAAAAAAAAAATTCT
5'*MSN5*RCS3R	GAAAGAAATAAAAAACAAATCAGACATGACTATTTGCTTTCTCTA
3'*MSN5*RCS3F	GAGAGAAGTAGACTGAACAAGTAATTATTGTGAAAAAAAAAATTC
3'*MSN5*DS	CGTCGACACCATTCAAATTCC

Table 7: Strains

Name	Genotype	Origin
WT	W303 (*MAT***a** *ade2 leu2 ura3 trp1-1 his3*)	Dichtl lab
ssu72-2	W303 *MAT***a** *ura3-1 trp1-1 ade2-1 leu2-3,112 his3-11,15 ssu72-2*)	Dichtl lab
Δrrp6	W303 (*MAT***a** *ade2 leu2 ura3 trp1-1 his3, Δrrp6::KANMX4*)	this study
ssu72-2 Δrrp6	W303 *MAT***a** *ura3-1 trp1-1 ade2-1 leu2-3,112 his3-11,15 ssu72-2, Δrrp6::KANMX4*)	this study
Δrco1	W303 (*MAT***a** *ade2 leu2 ura3 trp1-1 his3, Δrco1::KANMX4*)	this study
Δrco1 Δrrp6	W303 (*MAT***a** *ade2 leu2 ura3 trp1-1 his3, Δrco1::KANMX4, Δrrp6::TRP1*)	this study
Δrrp6 MSN5::ΔpARCS	W303 (*MAT***a** *ade2 leu2 trp1-1 his3,ura3::KANMX6, Δrrp6::TRP1, MSN5::ΔpARCS*)	this study
WT (YMH14)	*MATα cyc1-5000 cyc7-67 ura3-52 leu2-3,112 cyh2*	Hampsey lab
Δrrp6	*MATα cyc1-5000 cyc7-67 ura3-52 leu2-3,112 cyh2 rrp6::KANMX6*	this study
sua7-1(YMH124)	*MATα cyc1-5000 cyc7-67 ura3-52 leu2-3,112 cyh2 sua7-1*	Hampsey lab (*31*)
sua7-1 Δrrp6	*MATα cyc1-5000 cyc7-67 ura3-52 leu2-3,112 cyh2 sua7-1 rrp6::KANMX6*	this study
pta1-1	*MAT* **a** *pta1-1 ade2-1 leu2-Δ1 lys2 trp1-Δ101 ura3-52*	this study
pta1-1 Δrrp6	*MAT* **a** *pta1-1 ade2-1 leu2-Δ1 lys2 trp1-Δ101 ura3-52 rrp6::KANMX6*	this study
rna14-1	MATa *ade2-1 his3-11 leu2-3,112 trp1-1 ura3-1 rna14-1*	Kufel lab(*32*)
rna14-1 Δrrp6	MATa *ade2-1 his3-11 leu2-3,112 trp1-1 ura3-1 rna14-1 Δrrp6*	Kufel lab
rna15-2	MATa *ade2-1 his3-11 leu2-3,112 trp1-1 ura3-1 rna15-2*	Kufel lab(*32*)
rna15-2 Δrrp6	MATa *ade2-1 his3-11 leu2-3,112 trp1-1 ura3-1 rna15-2 Δrrp6*	Kufel lab

Table 8: Genomic data

Data	Comparison	P- value (wilcox-rank sum test)	Reference
H4 acetylation	Average H4 acetylation of SAT and CUT promoters in WT	6.7e-16	(*33*)
PolII occupancy	Average Rpo21 and Rpb3 occupancy of SRT and CUT promoters in WT	0.12 and 0.3	(*34*)
NFR size	NFR size of ORF having a CUT and SRT in WT	0.17	(*25*)
Isw2 occupancy	Average Isw2 occupancy of CUT and SRT in WT	0.48	(*35*)